Atomic Spectroscopy

Article

In Situ Carbon Isotope Microanalysis of Graphite by LA-MC-ICP-MS: Development of Reference Materials and Mass Loading Correction

Jue Lu,[a,b] Wei Chen,[b,*] Guoqi Liu,[c] Kui-Dong Zhao,[b] Shao-Yong Jiang,[b] Zhi-Yong Zhu,[a] and Xiang-Kun Zhu[a]

[a] State Key Laboratory of Deep Earth and Mineral Exploration, MNR Key Laboratory of Isotope Geology, Institute of Geology, Chinese Academy of Geological Sciences, Beijing 100037, P. R. China

[b] State Key Laboratory of Geological Processes and Mineral Resources, China University of Geosciences, Wuhan 430074, P. R. China

[c] School of Earth and Planetary Sciences, East China University of Technology, Nanchang 330013, P. R. China

Received: *November 21, 2025;* ***Revised:*** *January 21, 2026;* ***Accepted:*** *January 24, 2026;* ***Available online:*** *January 24, 2026.*

DOI: 10.46770/AS.2025.113

ABSTRACT: Graphite can preserve crucial information related to the carbon cycle in metamorphic, magmatic, and hydrothermal systems. However, traditional bulk isotope analysis often obscures significant microscale heterogeneity. This study establishes a reliable protocol for in situ carbon isotope analysis of graphite using laser ablation multi-collector inductively coupled plasma mass spectrometry (LA-MC-ICP-MS). Two critical challenges were addressed: the mass loading effect and the scarcity of appropriate reference materials. Mass loading induces significant carbon isotope fractionation, with the $\delta^{13}C$ deviation showing a linear dependence on the $^{12}C^+$ intensity ratio of sample to standard ($^{12C^+}I_{sam}/^{12C^+}I_{std}$). This deviation intensifies as the ratio diverges from 1, surpassing |2‰| at values of 0.2 and 2.6. The application of a linear regression correction reduces the deviations at these extreme ratios (0.2 and 2.6) from over |2‰| to within 0.50‰. Commercial pencil leads were validated as cost-effective reference materials for the in situ C isotope analysis of graphite. The 2H grade exhibited excellent micro-scale homogeneity (0.30‰, 2SD), performing slightly better than pressed pellets of the United States Geological Survey graphite standard USGS24 (0.50‰, 2SD), and negligible inter-matrix fractionation between these two samples ($|\Delta\delta^{13}C| \leq 0.22‰$). Calibration of variable-grade pencil leads (2B to 6B) achieved precisions ranging from 0.12‰ to 0.58‰ (2SD), with deviations within 0.18‰ of IRMS values. The method provides high spatial resolution with sub-permil accuracy, enabling resolution of intra-crystalline $\delta^{13}C$ zoning in graphite. It offers a robust framework for reconstructing metamorphic temperature histories, tracing carbon sources, and investigating fluid-mediated carbon precipitation in geological systems.

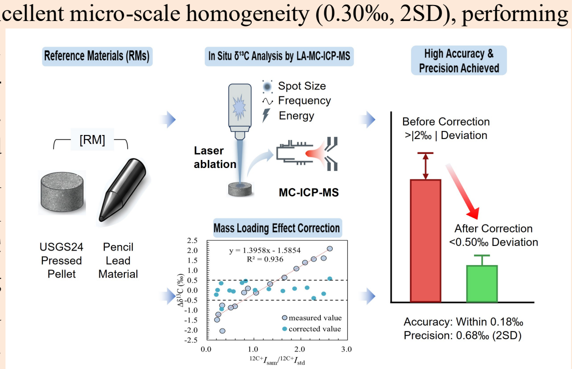

INTRODUCTION

Graphite is a minor but significant carbon reservoir in the Earth's crust. Its remarkable stability under crustal conditions makes it largely inert and an isolated archive, preserving unique information about deep carbon sources and processes that are distinct from the active carbon cycle at the surface. Graphite is conventionally categorized into three genetic types: magmatic, metamorphic, and hydrothermal.[1-5] Magmatic graphite crystallizes directly from silicate or carbonatite melts and occurs in igneous rocks as solid inclusions within fluid inclusions, interstitial crystals, or spherulites. Its carbon isotope composition exhibits limited intra-sample variation (<5‰), yet shows considerable regional heterogeneity, with $\delta^{13}C$ values typically ranging from –30‰ to –5‰, [6-8] as illustrated in Fig. 1. Metamorphic graphite, formed through the metamorphism of organic matter, generally displays a flaky morphology and spans a broad $\delta^{13}C$ range from –42‰ to –1‰, reflecting protolith heterogeneity and isotopic re-equilibration during high-grade metamorphism. Notably, distinct metamorphic lithologies (e.g., metapelites, schists and gneisses, granulites, and metabasic rocks) occupy characteristic isotopic intervals, further highlighting systematic compositional diversity.[6,7,9-13] Hydrothermal graphite precipitates directly from carbon-bearing fluids and exhibits diverse

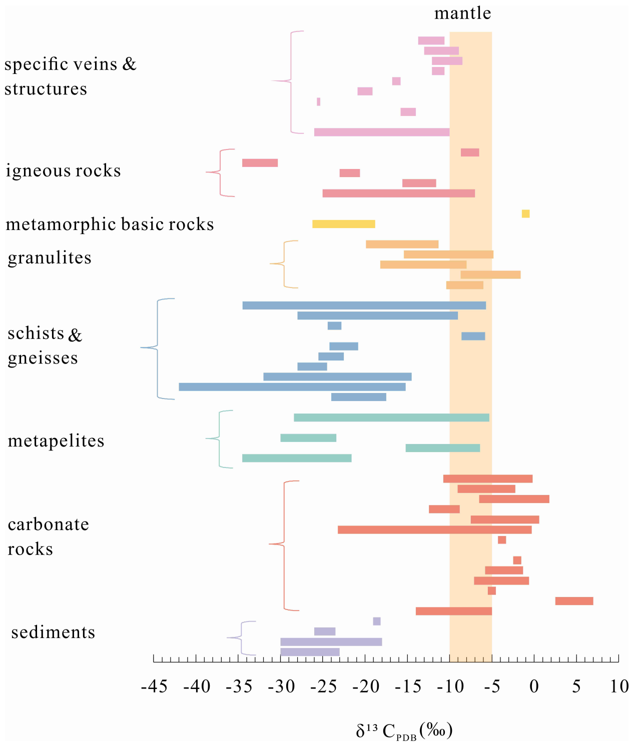

Fig. 1 Carbon isotope compositions of graphite from various geological settings. Classification is based on data from Hahn-Weinheimer and Hirner (1981),[6] Luque *et al.* (2012),[7] Safonov *et al.* (2018),[8] Satish-Kumar *et al.* (2011a, b),[9, 10] Vennemann and Smith (1992),[11] Valley and O'Neil (1981),[11] Ortega *et al.* (2010),[12] Yang *et al.* (2014),[13] Zuilen *et al.* (2003),[15] Peck *et al.* (2006),[16] and Rosing-Schow *et al.* (2017).[17] For detailed information, providing in the Supporting Information (Table S1).

crystal habits with pronounced spatial $\delta^{13}C$ heterogeneity, a variability attributed to complex fluid sources, precipitation environments, and influencing factors such as system openness, temperature, dominant carbon species (CO_2 vs. CH_4), and Rayleigh fractionation. These processes can produce systematic core-to-rim isotopic zoning within individual crystals.[9,10,14-17] The partial overlap in $\delta^{13}C$ values among the three genetic types underscores the complexity and occasional interplay of graphite-forming processes in different geological settings.

Carbon isotope fractionation in graphite is closely linked to temperature, oxidation state of the carbon phase, and reaction pathways. Experimental studies of the carbonate–graphite–CO_2 system have shown that fractionation decreases with increasing temperature, with high-temperature graphite typically enriched in ^{13}C and yielding $\delta^{13}C$ values close to those of the source carbon.[18,19] This temperature dependence forms the basis of the carbonate–graphite isotope thermometer, which is widely applied to constrain metamorphic temperatures and reconstruct thermal histories.[20,21] However, the accuracy of this thermometer depends on the robustness of the fractionation curve and the representativeness of the measured data, underscoring the importance of high precision in situ $\delta^{13}C$ analysis within graphite micro-domains.[19]

Conventional techniques such as gas-source isotope ratio mass spectrometry (IRMS) provide highly precise bulk $\delta^{13}C$ values but inherently average the isotopic composition of multiple graphite growth zones. This limitation hampers efforts to identify isotopic heterogeneity and resolve complex histories of graphite formation. To overcome this, in situ microanalytical techniques including Secondary Ion Mass Spectrometry (SIMS/ NanoSIMS), and Laser Ablation Multi-Collector Inductively Coupled Plasma Mass Spectrometry (LA-MC-ICP-MS) have been increasingly applied.[22-27] With a spatial resolution of 30 µm, SIMS analysis can achieve accuracy and precision within the sub per-mil (‰, 2SD) range for carbon isotopes.[22,23] However, SIMS is particularly sensitive to matrix effects caused by variations in sample composition (e.g., iron content in dolomite) and differences in structure (e.g., aragonite and calcite).[22,23] This sensitivity necessitates more stringent requirements for matrix-matched reference materials. The accuracy and precision of LA-MC-ICP-MS for measuring carbon isotopes are approximately 0.50‰ (2SD) with a spatial resolution of 90 µm.[22-27] This method offers several significant advantages relative to SIMS, including a lower instrument cost, high efficiency, straightforward operation, and relatively low analysis costs.

Despite these benefits, in situ $\delta^{13}C$ analysis of graphite by LA-MC-ICP-MS faces several challenges. During laser ablation analysis, graphite vaporizes to producing a mixture of gaseous and particulate carbon species. The proportions of these phases are influenced by both the characteristics of the matrix and the ablation parameters. These factors can lead to concentration-dependent elemental or isotopic fractionation, which may affect the analytical accuracy and reproducibility. Moreover, pronounced matrix effects exist between graphite and non-matched reference materials, particularly carbonates such as calcite.[26] At present, the scarcity of well-characterized graphite reference materials is a major limitation. With NBS-21 graphite powder no longer available, USGS24 is the only widely available certified graphite reference material.[28,29] For microanalytic techniques such as laser ablation, such certified powders are conventionally prepared as pressed pellets to meet the requirements for solid sampling. In this context, Zhang et al. (2024) [26] developed a LA-MC-ICP-MS protocol for in situ graphite $\delta^{13}C$ analysis under medium mass resolution. Their systematic investigation of signal-to-noise ratio, laser frequency, and calibration strategies demonstrated excellent reproducibility (2SD < 0.68 ‰) and strong agreement with IRMS data. Furthermore, the study also evaluated pressed pellets from the Lutang (LTSM) and Changshouyuan (CSY) deposits as potential in-house reference materials. These pellets not only showed high homogeneity (RSDs of ~0.030% for $^{13}C/^{12}C$ ratios) but also showed negligible matrix-dependent fractionation relative to natural graphite, confirming their practical utility for in situ microanalysis. Collectively, advancing in situ graphite isotope analysis depends on the continued development of homogeneous reference materials, together with improved correction schemes based on concentration–signal-to-noise relationships and carefully optimized standard–sample bracketing routines.

Given these constraints in reference material availability and method development, the application of LA-MC-ICP-MS for graphite carbon isotope analysis, while promising, still requires further refinement. Key challenges such as matrix effects, insufficiently constrained analytical parameters, and the scarcity of well-characterized graphite standards need to be systematically addressed. The present study therefore aims to evaluate LA-MC-ICP-MS protocols and test potential graphite reference materials, with the goal of establishing a robust in situ $\delta^{13}C$ method that combines high spatial resolution, accuracy, and broad applicability.

EXPERIMENTAL

Sample Description. Two categories of samples were employed to evaluate the in situ graphite carbon isotope analysis method (Fig. 2): (1) the international reference material USGS24 graphite powder supplied by the United States Geological Survey (USGS), and (2) commercially available pencil leads from the Chinese brand Marie's. These pencil leads consist of graphite blended with clay, wax, and other components to achieve specific physical properties that enable smooth gliding over surfaces while leaving a clear mark.[30]

USGS24 with a certified $\delta^{13}C_{VPDB}$ value of –16.05‰ ± 0.05‰,[28] was prepared for laser ablation analysis by compacting the original powder at 250 kN for over 5 min to form dense 11-mm-diameter pellet (Fig. 2). Commercial pencil leads spanning a range of hardness and blackness grades from 2H to 2B according to the HB standard nomenclature (where H denotes hardness and B indicates blackness, the latter corresponding to a higher graphite-to-clay ratio) were also examined. Bulk isotope analyses revealed that these pencil leads exhibit a relatively narrow $\delta^{13}C_{VPDB}$ range, from –21.83‰ to –21.10‰, rendering them suitable for assessing matrix effects and evaluating analytical reproducibility in laser ablation-based methods.

In situ carbon isotope analysis. In situ $\delta^{13}C$ measurements were conducted using a RESOlution 193 nm ArF excimer laser ablation system (Australian Scientific Instruments, Canberra) equipped with a two-volume ablation cell (Laurin Technic, Australia) coupled to a Nu Plasma II MC-ICP-MS (Nu Instruments, UK). Analyses were performed in single-spot mode, with carrier and auxiliary gases optimized to enhance signal stability and signal-to-noise ratio (SNR): 50–100 mL/min He, 1.05–1.10 L/min Ar, and 4 mL/min N_2. Laser parameters were systematically varied to assess their influence on isotopic results, including beam diameters (50–193 μm), repetition frequencies (4–20 Hz), and energy densities (1–5 J/cm²). Each analytical cycle consisted of 30 s of background acquisition followed by 40 s of sample ablation. Data were collected in Time-Resolved Analysis (TRA) mode, with 400 continuous integration cycles at 0.2 s per cycle. The instrumental settings and operating parameters are summarized in Table 1.

Fig. 2 Photographs of the two sample types used for in situ graphite carbon isotope analysis: a pressed pellet of USGS24 graphite reference material, and a set of commercial pencil leads (Marie's brand, hardness grades 2H to 8B).

Table 1. Operating conditions for MC-ICP-MS and laser ablation system

MC-ICP-MS (Nu Plasma)	Values
Cup-configuration	L4: ^{12}C; H7: ^{13}C
RF Power	1300 W
Cool gas flow	14.0 L/min
Auxiliary gas flow	0.8 L/min
Argon make-up gas flow	~1.05–1.10 L/min
Helium carrier gas flow	50–100 mL/min
Nitrogen gas flow	4 mL/min
sample cone	319-645 (1.15 mm orifice)
skimmer cone	Ni HS1-7 (0.6 mm orifice)
Mass resolution	low
Block number	1
Cycles of each block	400
Integration Time	0.2 s
Laser ablation system (RESOlution)	
Laser type	ArF excimer laser
Wavelength	193 nm
Pulse length	20 ns
Energy density	1–5 J/cm^2
Spot size	50–193 μm
Ablation mode	spot
Laser frequency	4–20 Hz

In situ C isotope data were corrected for instrumental mass bias using the standard–sample bracketing method, typically bracketing every 3–5 unknown analyses. To ensure comparability of the in situ $\delta^{13}C$ values obtained in this study with those of in-house reference materials, all results were recalculated relative to the internationally recognized VPDB (Vienna Pee Dee Belemnite) marine carbonate standard using the following equations:

$$\delta^{13}C = \left[\frac{(^{13}C/^{12}C)_{sample}}{(^{13}C/^{12}C)_{standard}} - 1\right] \times 1000 \quad (1)$$

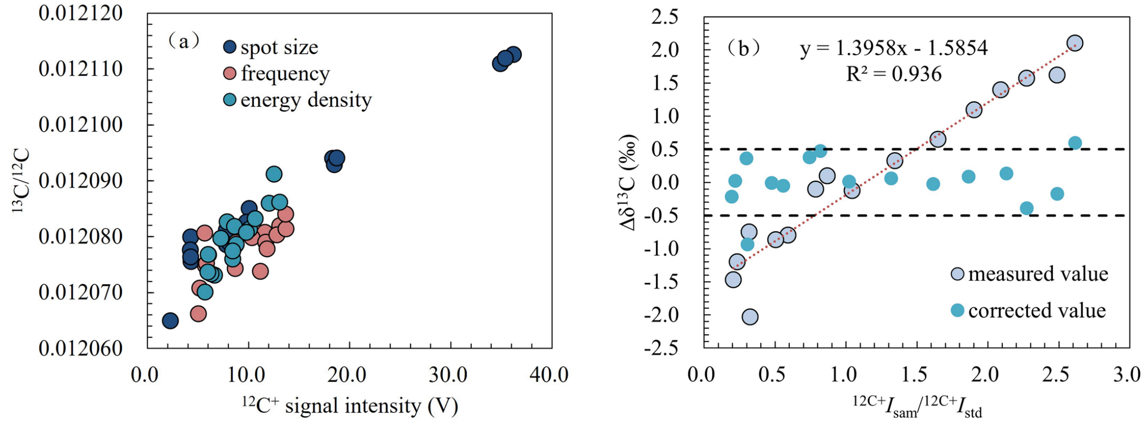

Fig. 3 Assessment of mass loading effects on in situ graphite $\delta^{13}C$ analysis by LA-MC-ICP-MS. (a) Measured $^{13}C/^{12}C$ ratio versus $^{12}C^+$ signal intensity, showing a positive correlation indicative of instrumental mass discrimination. (b) Deviation of laser ablation values from IRMS results ($\Delta\delta^{13}C$) as a function of the $^{12}C^+$ intensity ratio of sample to standard ($^{12C+}I_{sam}$ / $^{12C+}I_{std}$). The black dash line in (b) highlights the analytical deviation within ±0.50‰.

$$\delta^{13}C_{sample/VPDB} = \delta^{13}C_{sample/in\text{-}house\ RM} + \delta^{13}C_{in\text{-}house\ RM\ /VPDB} \quad (2)$$

where $\delta^{13}C_{sample/in\text{-}house\ RM}$ represents the measured δ-value of the sample relative to the in-house reference materials determined by LA-MC-ICP-MS, and $\delta^{13}C_{in\text{-}house\ RM\ /VPDB}$ denotes the δ-value of the in-house reference materials relative to VPDB, as determined by IRMS.

Determination of carbon isotopes for graphite samples. Bulk $\delta^{13}C$ values were determined using a Thermo Scientific DELTA V Advantage gas-source isotope ratio mass spectrometer (IRMS) coupled to an Elemental Analyzer (EA). Pencil lead samples (0.5–12 mg) were acid-treated, weighed, and encapsulated in 4 × 6 mm tin capsules prior to automated EA introduction. High-temperature combustion converted graphite to CO_2, which was purified sequentially through a $Mg(ClO_4)_2$ trap for H_2O removal and a 70 °C gas chromatographic (GC) column for separation of N_2 and other impurities. The purified CO_2 was then introduced into the IRMS for $\delta^{13}C$ measurement. Analytical precision, monitored using reference materials during the same batch, was better than ±0.1‰ (1σ).

RESULTS AND DISCUSSION

Effect of mass loading and correction approach. The dependence of instrumental mass discrimination on analyte signal intensity, commonly referred to as the mass loading effect, is a well-documented phenomenon in MC-ICP-MS isotope analysis.[31,32] For carbonaceous materials like graphite, variations in carbon signal intensity between the sample and the bracketing standard can arise from differences in intrinsic carbon content, it can also be affected by other factors, such as laser ablation yield, aerosol transport efficiency, or instrument drift. Such signal intensity mismatches, if not properly accounted for, compromise the accuracy of $\delta^{13}C$ determinations because the measured isotope ratios in the sample can be systematically biased relative to the standard.

To systematically evaluate this effect, laser parameters including beam diameter (50–193 μm), repetition frequency (4–20 Hz), and energy density (1–5 J cm^{-2}) were changed using a single pencil lead sample. This approach modulated the amount of carbon introduced into the plasma, thereby simulating concentration differences and enabling a robust assessment of their impact on measured $\delta^{13}C$ values. The results (Fig. 3a) reveal a pronounced positive linear correlation between the measured $^{13}C/^{12}C$ ratio and the $^{12}C^+$ signal intensity (ranging from 2.28 to 36.21 V), indicating apparent heavy-isotope enrichment at higher signal intensities. The $^{13}C/^{12}C$ ratio increased from 0.011265 to 0.011612, corresponding to a significant shift in $\delta^{13}C$ of approximately +31‰. Notably, datasets acquired under different ablation conditions but within equivalent intensity ranges (<16 V) exhibited consistent isotopic trends (Fig. 3a). This indicates that the dominant fractionation mechanism does not occur during the laser ablation process itself, but rather during subsequent stages of ion generation, extraction, and transmission within the ICP-MS source.[26] This behavior can be explained by ion-beam dynamics and space-charge effects. During the expansion of the plasma through the sampler–skimmer interface, ions undergo supersonic acceleration.[33-36] Lighter ^{12}C ions, having lower momentum, are more susceptible to scattering through collisions with residual Ar neutrals and to radial displacement under space-charge forces. In contrast, heavier ^{13}C ions are preferentially transmitted along the beam axis, resulting in an apparent enrichment of the heavy isotopes. Similar mass-dependent spatial distribution effects have been observed in boron isotope studies using MC-ICP-MS,[37] suggesting a generalized mechanism for light-element isotopes characterized by large relative mass differences ($\Delta m/m$). In essence, the observed mass loading effect reflects the complex interplay among kinetic energy distributions, collision cross-sections, and Coulomb interactions of C ions within the expanding ion plume.

To quantitatively express the signal intensity disparity between the sample and the standard, we define the signal intensity ratio as follows:

$$^{12C^+}I_{sam}/^{12C^+}I_{std} = \frac{^{12C^+}I_{sam}}{(^{12C^+}I_{std\text{-}1} + ^{12C^+}I_{std+1})/2} \tag{3}$$

Where $^{12C^+}I_{sam}$ is the $^{12}C^+$ signal intensity of the sample, and the $^{12C^+}I_{std}$ is the average $^{12}C^+$ signal intensity of the two bracketing standard measurements immediately preceding ($^{12C^+}I_{std\text{-}1}$) and following the sample ($^{12C^+}I_{std+1}$). This ratio fundamentally represents the relative difference in carbon load between the sample and the standard.

As illustrated in Fig. 3b, the deviation of $\delta^{13}C$ ($\Delta\delta^{13}C$) between LA-MC-ICP-MS and IRMS measurements exhibits a strong linear dependence on the $^{12C^+}I_{sam}/^{12C^+}I_{std}$ ratio. A deviation in ratios of 1 ± 0.6 from unity can introduce a bias exceeding 0.60‰ in $\delta^{13}C$, with deviations surpassing |2‰| at ratios values of 0.2 and 2.6. Restricting $^{12C^+}I_{sam}/^{12C^+}I_{std}$ to the range of 0.5–2.0 effectively confines analytical deviations to within ±1‰. These results underscore the critical importance of signal intensity matching between standards and samples during standard–sample bracketing to achieve high-precision carbon isotope analysis.

Mitigating this intensity mismatch effect is essential for accurate isotope analysis. Previous studies have commonly employed one of two approaches: (1) rigorous matching of analyte concentrations between samples and standards, or (2) instrumental tuning to minimize sensitivity drift.[38] The former approach can be challenging for natural samples with diverse compositions, while the latter often lacks long-term stability and reproducibility. In laser ablation analysis, signal intensity can be practically modulated by adjusting laser parameters (*e.g.*, spot size, repetition rate, and energy density) to ablate controlled amounts of material. As demonstrated earlier, such parameter variations do not induce carbon isotope fractionation, making this a viable strategy for intensity matching.

Alternatively, the effect of intensity mismatch can be corrected mathematically. This approach is adapted from methods previously established for iron and potassium isotope analysis.[38,39] The correction relies on a calibration curve constructed by analyzing (1) a single standard at varying signal intensities achieved by modulating laser parameters, or (2) a set of different standards/samples with inherent concentration variations. Both approaches simulate a range of $^{12C^+}I_{sam}/^{12C^+}I_{std}$ values. The well-defined linear relationship between $^{12C^+}I_{sam}/^{12C^+}I_{std}$ and isotope bias enables the use of the following expression:

$$\delta^{13}C_{corrected} = \delta^{13}C_{measured} - (a*R + b) \tag{4}$$

where R is the signal intensity ratio defined in Equation (3). In the present study, the fitted function was $y = 1.3958x - 1.5854$ ($R^2 = 0.936$). Application of this regression model effectively reduces residual deviations to within 0.50‰ (Fig. 3b), offering a robust strategy to correct for mass-loading effects and significantly improve analytical accuracy. Such a correction curve should be established at the beginning of any extended analytical run or after any instrument tuning.

Candidate reference materials for in situ graphite carbon isotope analysis. The establishment of robust reference materials (RMs) is central to advancing in situ carbon isotope analysis of graphite. In isotope geochemistry, the reliability of data hinges not only on instrument performance but also on the use of well-characterized, homogeneous standards that enable accurate calibration and inter-laboratory comparability.[40] While numerous carbonate and silicate RMs exist for oxygen and carbon isotopes, graphite has long lacked certified materials suitable for microanalysis.[29] This shortage is particularly acute for in situ microanalysis, with only a limited number of proposed candidates, such as the pressed powder pellets LTSM and CSY, reported by Zhang *et al.* (2024).[26] This study therefore assessed two practical and readily available alternatives: pellet prepared from USGS24 graphite powder and commercial pencil leads of varying hardness grades.

USGS24 graphite pellet. USGS24 is the only internationally certified graphite isotope standard, with a $\delta^{13}C_{VPDB}$ value of −16.05‰ ± 0.05‰. Traditionally distributed as a fine powder, its adaptation to laser ablation requires compaction into solid pellets. Here, USGS24 powder was pressed under 250 kN to form dense 11 mm pellets. Micro-scale isotopic homogeneity was evaluated using the standard–sample bracketing protocol, with 30 ablation spots arranged in a cross-pattern. Measured $^{12}C^+$ intensities ranged from 8.00 to 10.09 V, with $\delta^{13}C$ reproducibility of 0.50‰ (2SD; Fig. 4a), comparable to the approximately 0.60‰ (2SD) reported for LTSM and CSY by Zhang *et al.* (2024).[26] Minor fluctuations likely reflect residual density gradients and micro-porosity from pelletization, consistent with earlier observations that compaction-induced heterogeneities can affect ablation yield.[41] Nevertheless, the reproducibility achieved here indicates that pressed USGS24 pellets satisfy the baseline requirements for in situ calibration. Moreover, the work of Zhang *et al.* (2024)[26] demonstrates that the carbon isotope fractionation between such pressed powder pellets and natural graphite is negligible, underscoring the broad applicability of the USGS24 pellet for microanalysis.

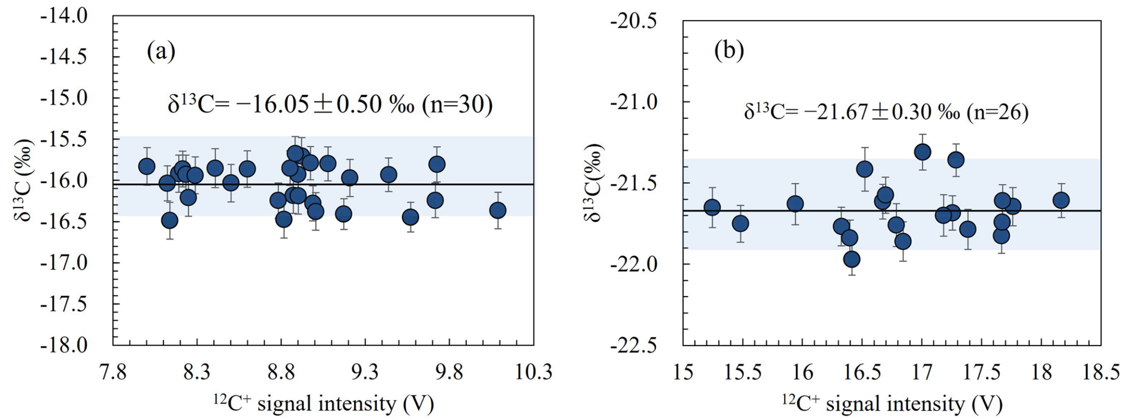

Fig. 4 Evaluation of carbon isotope homogeneity in candidate reference materials for in situ graphite analysis. (a) USGS24 pressed powder pellet; (b) 2H commercial pencil lead. The Error bars represent the internal precision (2SE), while the solid line and grey field indicates the obtained average and reproducibility (2SD), respectively.

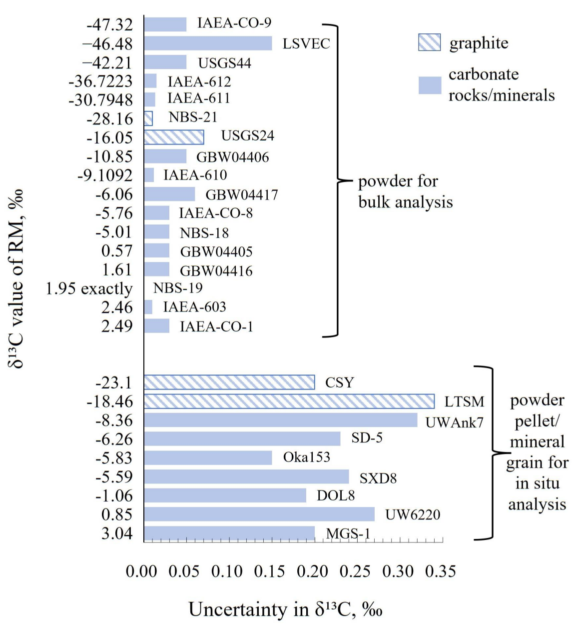

Fig. 5 Compilation of reported $\delta^{13}C$ values and associated uncertainties (1SD) for carbon-bearing reference materials. Data are from published sources and Chinese National Standard Material Resource Sharing Platform.[23-26,28,42-47] For detailed information, providing in the Supporting information (Table S2).

Commercial pencil leads. Industrially produced pencil leads offer an unconventional yet promising alternative compared to the USGS24, LTSM and CSY pellets. Our IRMS characterization of Chinese "Marie's" brand leads (grades 2H, 2B, 4B, 6B, 8B) revealed an unusually narrow bulk $\delta^{13}C_{VPDB}$ range from –21.83‰ to –21.10‰. This compositional uniformity likely reflects the large-scale blending of natural graphite sources during manufacturing, which homogenizes the C isotopic variability. Moreover, the widespread commercial availability and low cost of these materials make them attractive candidates for routine laboratory use.

To evaluate carbon isotope homogeneity, 26 ablation spots were analyzed on the 2H pencil lead, revealing a $\delta^{13}C$ reproducibility of 0.30‰ (2SD; Fig. 4b), which confirms excellent isotopic uniformity across the pencil lead surface. This high level of homogeneity can be attributed to the industrial processing of synthetic graphite, which removes volatiles and enhances structural consistency. Although minor clay binders are added to improve mechanical stability, which reduces the risk of pellet crumbling or surface irregularities during ablation, they do not significantly influence the $\delta^{13}C$ composition. Furthermore, in a reciprocal calibration experiment using standard–sample bracketing with the 2H pencil lead (IRMS-determined $\delta^{13}C_{VPDB}$ = –21.69‰) and USGS24 graphite pellets (certified $\delta^{13}C_{VPDB}$ = –16.05‰) alternately serving as standard and unknown, the laser-ablation measured values were –16.10 ± 0.30‰ (2SD, n = 4) for USGS24 and –21.47 ± 0.42‰ (2SD, n = 4) for the 2H pencil (Fig. 6b). The deviations from the reference values (only 0.05‰ and 0.22‰, respectively) are negligible, indicating that matrix-dependent fractionation is insignificant between these graphite forms. These properties, combined with their isotopic consistency, suggest that 2H pencil leads may serve as high-quality "community standards" for LA-MC-ICP-MS graphite studies.

The assessment of USGS24 pellets and commercial pencil leads underscores the ongoing challenge of reference material availability in carbon isotope geochemistry. As summarized in Fig. 5, carbon-bearing reference materials cover a broad $\delta^{13}C$ spectrum and are available in various physical forms, ranging from powders for bulk analysis to pressed pellets or mineral grains suitable for in situ microanalysis.[23-26,28,42-47] Their associated uncertainties are generally below 0.10‰ (1SD) for bulk and 0.35‰ (1SD) for in situ

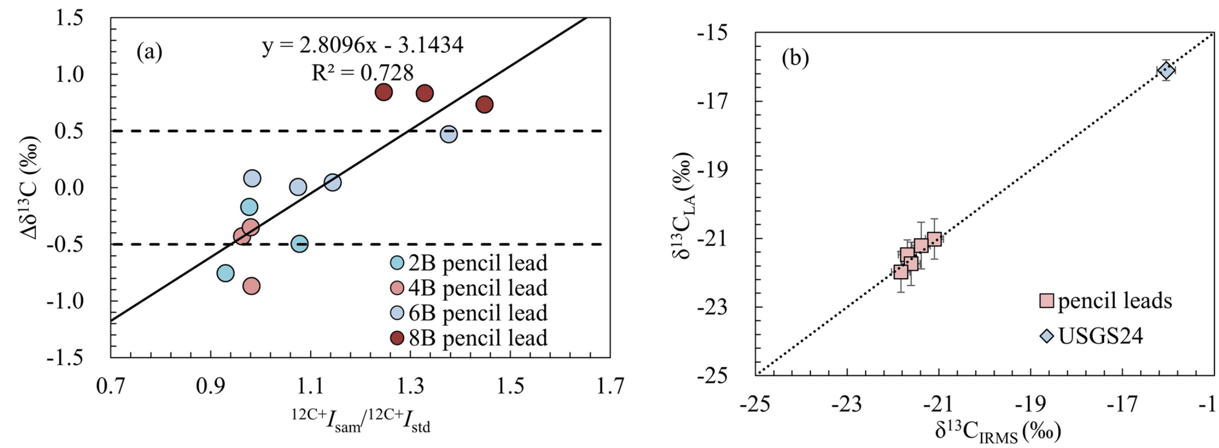

Fig. 6 Evaluation of analytical accuracy and mass loading correction for pencil leads and USGS24. (a) Deviation between LA-MC-ICP-MS and IRMS results of pencil leads ($\Delta\delta^{13}C$) as a function of the ${}^{12C^+}I_{sam}/{}^{12C^+}I_{std}$ ratio. The solid line represents the linear regression ($y = 2.8096x - 3.1434$, $R^2 = 0.728$) used to correct for mass loading effects. (b) Comparison of $\delta^{13}C$ values obtained by LA-MC-ICP-MS after linear correction and conventional IRMS. Error bars represent ±2SD reproducibility, and the dash line denotes 1:1 agreement.

measurements. Within this context, graphite-specific reference materials remain particularly scarce. Nevertheless, this study, together with recent efforts by Zhang *et al.* (2024),[26] has expanded the range of practical options: USGS24 pellets provide metrological traceability as an internationally certified material; commercial pencil leads deliver high mechanical cohesion, excellent microscale homogeneity, and are cost-effective and widely accessible; and laboratory-developed pellets such as LTSM and CSY serve as well-characterized in-house candidates with documented homogeneity.

Accuracy and precision of in situ graphite carbon isotope analysis. To further test applicability, the homogeneous 2H pencil was used to calibrate $\delta^{13}C$ values of other commercial pencil grades. The results showed good overall agreement with IRMS data (Table S3; Fig. 6a), with average $\Delta\delta^{13}C$ values of –0.48‰ for 2B, –0.55‰ for 4B, and +0.15‰ for 6B, and precisions between 0.12‰ and 0.58‰ (2SD). The 8B grade exhibited a larger initial deviation of +0.80‰, which is also attributable to mass loading effects, as indicated by its higher ${}^{12C^+}I_{sam}/{}^{12C^+}I_{std}$ ratio relative to the 2H standard (Fig. 6a), which likely reflects decreased hardness and higher graphite-to-clay ratio. Importantly, all $\Delta\delta^{13}C$ values show a clear linear dependence on the ${}^{12C^+}I_{sam}/{}^{12C^+}I_{std}$ ratio, following the regression function $y = 2.8096x - 3.1434$ ($R^2 = 0.728$). After applying this correction, the $\delta^{13}C$ values of all pencil leads, including the 8B grade, align closely with IRMS results, with post-correction deviations within |0.18‰| (Table S3; Fig. 6b). This confirms that the method, especially when combined with linear regression correction, achieves accuracy within the acceptable threshold of ≤0.50‰ for in situ carbon isotope analysis of graphite.

Due to the low atomic mass of carbon and the low natural abundance of ^{13}C (~1.1%), the ^{13}C signal is inherently weak, making measurement reproducibility highly dependent on the signal-to-noise ratio (SNR).[24-26] As a result, LA-MC-ICP-MS analysis of carbon isotopes is more sensitive to plasma stability and detector linearity compared with heavier isotope systems such as Sr or Pb. Our results show that internal precision better than 0.20‰ (2SE) can be achieved when the SNR exceeds 2.5 (Fig. 7), highlighting the critical role of optimized ion transmission and plasma stability. These conditions are strongly influenced by the use of high-purity gas supplies, which help minimize background noise and enhance signal robustness.[48-50]

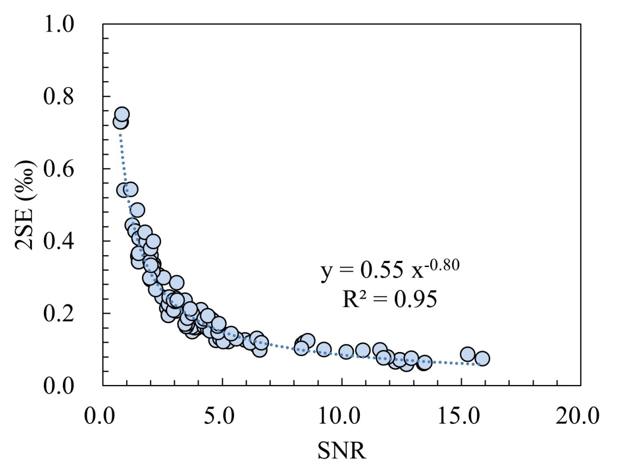

Fig. 7 Relationship between signal-to-noise ratio (SNR) and internal precision (2SE) of in situ $\delta^{13}C$ measurements. The fitted power-law curve $y = 0.55x^{-0.80}$ with a high coefficient of determination ($R^2 = 0.95$) illustrates that precision improves markedly as SNR increases.

The combined uncertainty associated with the corrected $\delta^{13}C$ values ($\delta^{13}C_{corrected}$) was estimated by propagating the main sources of variability, including the internal precision of individual LA-MC-ICP-MS measurements, the reproducibility of the reference material used for calibration, and the uncertainty introduced by the mass-loading correction model itself.

The uncertainty of $\delta^{13}C_{corrected}$ was calculated using the following error propagation formula, which accounts for the linear correction model $\delta^{13}C_{corrected} = \delta^{13}C_{measured} - (a \times R + b)$:

$$U(\delta^{13}C_{corrected}) = \sqrt{U(\delta^{13}C_{measured})^2 + [a \cdot U(R)]^2} \quad (5)$$

Where $U(\delta^{13}C_{corrected})$ is the uncertainty of the measured $\delta^{13}C$ value, taken as the internal precision. $U(R)$ is the uncertainty in the signal intensity ratio R. Using representative values from the calibration session, the combined expanded uncertainty (k = 2, approximately 95% confidence level) for $\delta^{13}C_{corrected}$ was estimated to be better than ±0.68‰. This value encompasses both the precision of the measurement and the uncertainty introduced by the correction process, confirming that the method maintains sub-permil accuracy suitable for resolving natural $\delta^{13}C$ variations in graphite.

Natural graphite deposits generally exhibit $\delta^{13}C$ ranges between 5 and 10‰, with some crystals from partially melted metamorphic rocks showing intra-crystalline zoning that exceeds 1‰ (Fig. 1).[9,10] The method developed in this study provides the necessary resolution to differentiate among organic, mantle, and carbonate-derived carbon sources. It also enables tracking of fluid-evolution pathways and the identification of isotopic zoning within individual graphite grains.

CONCLUSION

This study established an in situ analysis method for graphite carbon isotopes using LA-MC-ICP-MS, successfully overcoming two major challenges: the mass loading effect and the scarcity of suitable calibration materials. Our results demonstrate a clear positive correlation between signal intensity and measured $\delta^{13}C$ values. By defining a signal intensity matching threshold, where the ${}^{12}C^{+}I_{sam}$ / ${}^{12}C^{+}I_{std}$ ratio is maintained near 1 through modulation of laser parameters (*e.g.*, spot size, frequency, energy density), deviations between LA and IRMS results were effectively constrained. Further enhancement of analytical accuracy was achieved through a linear regression correction. The Marie's 2H commercial pencil lead proved to be an excellent candidate reference material, exhibiting micro-scale homogeneity (0.30‰, 2SD) slightly over pressed USGS24 pellets (0.50‰, 2SD). Reciprocal calibration between these materials indicated negligible inter-matrix fractionation ($|\Delta\delta^{13}C| \leq 0.22$‰). The integration of standard-sample bracketing with the linear regression mass loading correction yields a final method precision of 0.68‰ (2SD) and an accuracy within 0.18‰.

ASSOCIATED CONTENT

The supporting information (Tables S1) is available at https://www.at-spectrose.com.

AUTHOR INFORMATION

Wei Chen received her BSc degree in Environmental Science from Nanjing University in 2010, and her PhD in Geology from the University of Notre Dame, USA, in 2014. She is currently a Professor of Geochemistry and Economic Geology at China University of Geosciences (Wuhan). Her research focuses on carbonatites and alkaline rocks, their associated critical metal resources, and the development of microanalytical techniques. Wei Chen is the author or co-author of over 60 peer-reviewed scientific articles, with an h-index of 30 (ResearchGate). She has served as a Council Member of the International Association of Geoanalysts since 2022.

Corresponding author

* W. Chen

E-mail address: wchen@cug.edu.cn

Notes

The authors declare no competing financial interest.

ACKNOWLEDGMENTS

We are grateful to Bin Hu for his insightful comments on this study. This work was financially supported by the National Natural Science Foundation of China (42303026, 42321001), the Postdoctoral Fellowship Program of the China Postdoctoral Science Foundation (GZC20232465), the Central Government Guided Local Science and Technology Development Project of Hubei Province (2025CSA006) and the State Key Laboratory of Geological Processes and Mineral Resources, China University of Geosciences (GPMR-2025-QT02).

REFERENCES

1. J. A. Jaszczak, G. W. Robinson, S. Dimovski, and Y. Gogotsi, *Carbon*, 2003, **41**, 2085-2092. https://doi.org/10.1016/S0008-6223(03)00214-8
2. J. A. Jaszczak, S. Dimovski, S. A. Hackney, G. W. Robinson, P. Bosio, and Y. Gogotsi, *Can. Mineral.*, 2007, **45**, 379-389. https://doi.org/10.2113/gscanmin.45.2.379
3. A. G. Doroshkevich, F. Wall, and G. S. Ripp, *Contrib. Mineral. Petrol.*, 2007, **153**, 339-353. https://doi.org/10.1007/s00410-006-0150-z
4. J. F. Barrenechea, F. J. Luque, D. Millward, L. Ortega, O. Beyssac, and M. Rodas, *Contrib. Mineral. Petrol.*, 2009, **158**, 37-51.

https://doi.org/10.1007/s00410-008-0369-y

5. C. Pérez-Soba, C. Villaseca, and A. Fernández, *Am. Mineral.*, 2017, **102**, 728-742. https://doi.org/10.2138/am-2017-5895.

6. P. Hahn-Weinheimer and A. Hirner, *Geochem. J.*, 1981, **15**, 9-15. https://doi.org/10.2343/geochemj.15.9

7. F. J. Luque, E. Crespo-Feo, J. F. Barrenechea, and L. Ortega, *Geosci. Front.*, 2012, **3**, 197-207. https://doi.org/10.1016/j.gsf.2011.11.006

8. G. Safonov, V. N. Reutsky, D. A. Varlamov, V. O. Yapaskurt, M. A. Golunova, V. D. Shcherbakov, D. D. van Reenen, A. C. Smit, and V. G. Butvina, *Gondwana Res.*, 2018, 60, 129-152. https://doi.org/10.1016/j.gr.2018.04.009

9. M. Satish-Kumar, J. A. Jaszczak, T. Hamamatsu, and H. Wada, *Am. Mineral.*, 2011, **96**, 470-485. https://doi.org/10.2138/am.2011.3576

10. M. Satish-Kumar, H. Yurimoto, S. Itoh, and B. Cesare, *Contrib. Mineral. Petrol.*, 2011, **162**, 821-834. https://doi.org/10.1007/s00410-011-0626-3

11. T. W. Vennemann and H. S. Smith, *Precambrian Res.*, 1992, **55**, 365-397. https://doi.org/10.1016/0301-9268(92)90035-M.

12. L. Ortega, D. Millward, F. J. Luque, J. F. Barrenechea, O. Beyssac, J. M. Huizenga, M. Rodas, and S. M. Clarke, *Geochim. Cosmochim. Acta*, 2010, **74**, 2429-2449. https://doi.org/10.1016/j.gca.2010.01.020.

13. Q. Y. Yang, M. Santosh, and H. Wada, *Precambrian Res.*, 2014, **255**, 641-652. https://doi.org/10.1016/j.precamres.2014.04.005

14. M. Santosh, H. Wada, M. Satish-Kumar, and S.S. Binu-Lal, *Am. Mineral.*, 2003, **88**, 1689-1696. https://doi.org/10.2138/am-2003-11-1208

15. M. A. V. Zuilen, A. Lepland, J. Teranes, J. Finarelli, M. Wahlen, and G. Arrhenius, *Precambrian Res.*, 2003, **126**, 331-348. https://doi.org/10.1016/S0301-9268(03)00103-7

16. W. H. Peck, R. A. Volkert, M. T. Meredith, and E. L. Rader, *J. Geol.*, 2006, **114**, 485-499. https://doi.org/10.1086/504181.

17. N. Rosing-Schow, L. Bagas, J. Kolb, T. Balić-Zunić, C. Korte, and M. L. Fiorentini, *Miner. Deposita*, 2017, **52**, 769-789. https://doi.org/10.1007/s00126-016-0701-9.

18. N. Scheele and J. Hoefs, Contrib Mineral Petrol, 1992, **112**, 35-45. https://doi.org/10.1007/BF00310954

19. N. Kueter, M. D. Lilley, M. W. Schmidt, and S. M. Bernasconi, *Geochim. Cosmochim. Acta*, 2019, **253**, 290-306. https://doi.org/10.1016/j.gca.2019.03.020

20. J. W. Valley and J. R. O'Neil, *Geochim. Cosmochim. Acta*, 1981, **45**, 411-419. https://doi.org/10.1016/0016-7037(81)90249-0

21. S. R. Dunn and J. W. Valley, J. Metamorph. *J. Metamorph. Geol.*, 1992, **10**, 487-501. https://doi.org/10.1111/j.1525-1314.1992.tb00100.x

22. C. Rollion-Bard, D. Mangin, and M. Champenois, *Geostand. Geoanal. Res.*, 2007, **31**, 39-50. https://doi.org/10.1111/j.1751-908X.2007.00834.x

23. M. G. Śliwiński, K. Kitajima, R. Kozdon, M. J. Spicuzza, J. H. Fournelle, A. Denny, and J. W. Valley, *Geostand. Geoanal. Res.*, 2016, **40**, 173-184. https://doi.org/10.1111/ggr.12118

24. W. Chen, J. Lu, S. Y. Jiang, K. D. Zhao, and D. F. Duan, *Anal. Chem.*, 2017, **89**, 13415-13421. https://doi.org/10.1021/acs.analchem.7b03678

25. J. Lu, W. Chen, W. Zhang, H. Liu, A. Simonetti, Z. C. Hu, Y. S. Liu, K. D. Zhao, and S. Y. Jiang, *J. Anal. At. Spectrom.*, 2022, **37**, 278-288. https://doi.org/10.1039/d1ja00356a

26. J. Zhang, C. Li, X. Li, W. Wang, P. Yu, L. Zhou, and W. Qu, *J. Anal. At. Spectrom.*, 2024, **39**, 800-807. https://doi.org/10.1039/D3JA00402C

27. Y. M. Huo, Z. Y. Zhu, C. F. Fan, Y. W. She, J. L. Hao, and X. K. Zhu, *J. Anal. At. Spectrom.*, 2025, **40**, 700-714. https://doi.org/10.1039/d4ja00554c

28. T. B. Coplen, W. A. Brand, M. Gehre, M. Gröning, H. A. J. Meijer, B. Toman, and R. M. Verkouteren, *Anal. Chem.*, 2006, **78**, 2439-2441. https://doi.org/10.1021/ac052027c.

29. W. A. Brand, T. B. Coplen, J. Vogl, M. Rosner, and T. Prohaska, *Pure Appl. Chem.*, 2014, **86**, 425-467. https://doi.org/10.1515/pac-2013-1023

30. C. Black, C. Poile, J. Langley, and J. Hermiman, *Rapid Commun. Mass Spectrom.*, 2006, **20**, 1053-1060. https://doi.org/10.1002/rcm.2408

31. L. Yang, S. Tong, L. Zhou, Z. Hu, Z. Mester, and J. Meija, *J. Anal. At. Spectrom.*, 2018, **33**, 1849-1861. https://doi.org/10.1039/C8JA00210J.

32. W. J. Li, Y. Zhao, B. X. Su, B. Y. Gao, J. Wang, and S. K. Liu, *J. Anal. At. Spectrom.*, 2023, **38**, 603-608. https://doi.org/10.1039/d3ja00022b

33. K. G. Heumann, S. M. Gallus, G. Rädlinger, and J. Vogl, *J. Anal. At. Spectrom.*, 1998, **13**, 1001-1008. https://doi.org/10.1039/A801965G

34. G. H. Fontaine, B. Hattendorf, B. Bourdon, and D. Günther, *J. Anal. At. Spectrom.*, 2009, **24**, 637-648. https://doi.org/10.1039/b816948a

35. N. Kivel, I. Günther-Leopold, F. Vanhaecke, and D. Günther, *Spectrochim. Acta B*, 2012, **76**, 126-132. https://doi.org/10.1016/j.sab.2012.06.045

36. W. Zhang and Z. Hu, *Spectrochim. Acta B*, 2020, **171**, 105929. https://doi.org/10.1016/j.sab.2020.105929.

37. L. Lin, Z. C. Hu, L. Yang, W. Zhang, Y. S. Liu, S. Gao, and S. H. Hu, *Chem. Geol.*, 2014, **386**, 22-30. https://doi.org/10.1016/j.chemgeo.2014.08.001

38. X. Y. Zheng, X. Y. Chen, W. Ding, Y. Zhang, S. Charin, and Y. Gérard, *J. Anal. At. Spectrom.*, 2022, **37**, 1273-1287. https://doi.org/10.1039/d2ja00078k

39. F. Albarède and B. Beard, *Rev. Mineral. Geochem.*, 2004, **55**, 113-152. https://doi.org/10.2138/gsrmg.55.1.113

40. T. Meisel and J. S. Kane, *Accred. Qual. Assur.*, 2011, **16**, 407-414. https://doi.org/10.1007/s00769-011-0802-1.

41. J. Lu, W. Chen, H. Y. Jin, J. Jiang, J. Lin, A. Yang, M. Li, K. D. Zhao, S.Y. Jiang, and Y. S. Liu, *J. Anal. At. Spectrom.*, 2024, **39**, 820-828. https://doi.org/10.1039/d3ja00385j

42. M. Schoell, E. Faber, and M. L. Coleman, *Org. Geochem.*, 1983, **5**, 3-6. https://doi.org/10.1016/0146-6380(83)90010-4

43. G. Hut, Consultants' Group Meeting on Stable Isotopic Reference Samples for Geochemical and Hydrological Investigations. Vienna, International Atomic Energy Agency, 1987. https://inis.iaea.org/records/t7hgm-7h428

44. W. Stichler, Reference and intercomparison materials for stable isotopes of light elements. Vienna, International Atomic Energy Agency, 1995. https://www.iaea.org/publications/5471/reference-and-intercomparison-materials-for-stable-isotopes-of-light-elements

45. S. Assonov, A. Faigelj, J. F. Hélie, C. Allison, and M. Gröning, *Rapid Commun. Mass Spectrom.*, 2021, **35**, e9014. https://doi.org/10.1002/rcm.9014

46. S. Assonov, M. Groening, A. Fajgelj, J. F. Hélie, and C. Hillaire-Marcel, *Rapid Commun. Mass Spectrom.*, 2020, **34**, e8867. https://doi.org/10.1002/rcm.8867

47. H. P. Qi, H. Moossen, H. A. J. Meijer, T. B. Coplen, A. T. Aerts-Bijma, L. Reid, H. Geilmann, J. Richter, M. Rothe, W. A. Brand, B.

Toman, J. Benefield, and J. F. Hélie, *Rapid Commun. Mass Spectrom.*, 2021, **35**, e9006. https://doi.org/10.1002/rcm.9006.

48. D. Günther and C. A. Heinrich, *J. Anal. At. Spectrom.*, 1999, **14**, 1369-1374. https://doi.org/10.1039/A901649J
49. Z. C. Hu, S. Gao, Y. S. Liu, S. H. Hu, H. H. Chen, and H. L. Yuan, *J. Anal. At. Spectrom.*, 2008, **23**, 1093-1101. https://doi.org/10.1039/b804760j
50. J. Lu, W. Chen, F. Yang, Q. L. Li, K. D. Zhao, and S. Y. Jiang, *Talanta*, 2025, **285**, 127371, https://doi.org/10.1016/j.talanta.2024.127371.